Journal of Inorganic and General Chemistry

ZAAC

Zeitschrift für anorganische und allgemeine Chemie

Accepted Article

Title: Crystal structure of N-(1,3-benzothiazol-2-yl)-4-iodobenzene-1-sulfonohydrazide: the importance of unusual N-H···π and I···π interactions on the supramolecular arrangement.

Authors: Lígia Maria da Silva Rebelo Gomes, Herbert Früchtl, John N. Low, Tanja van Mourik, Alessandra C. Pinheiro, Marcus V. N. de Souza, and James L. Wardell

To be cited as: *Z. anorg. allg. Chem.* **2022**, e202200087

Link to VoR: https://doi.org/10.1002/zaac.202200087

WILEY-VCH

www.zaac.wiley-vch.de

10.1002/zaac.202200087

ARTICLE

WILEY-VCH

Crystal structure of N-(1,3-benzothiazol-2-yl)-4-iodobenzene-1-sulfonohydrazide: the unexpected importance of I N-H···π and I···π interactions on the supramolecular arrangement.

Lígia R. Gomes, * [b,c] Herbert Früchtl,[a] John N. Low, * [d] Tanja van Mourik,[a] Alessandra C. Pinheiro [e], Marcus V. N. de Souza,[e] James L. Wardell [c,d]

On the occasion of the 80th Birthday of Professor Dr. Dieter Fenske

Abstract: The 2-hydrazinyl-1,3-benzothiazole derivatives are precursors for synthesis of several compounds of technological interest, including the Bt-NH-N=CHR$_1$ (R$_1$ = alkyl, aryl, heteroaryl), derivatives. Usually when Bt-NH-NH$_2$ is allowed to react with a benzenesulfonyl chloride the substitution is observed in the terminal nitrogen of the arenehydrazine unit, but when 4-iodophenyl sulfonyl chloride (4-IC$_6$H$_4$SO$_2$Cl) was used, the product isolated was the title compound as confirmed by Rx-analysis.

The determination of the crystal structure revealed that the definition of the arrangement was driven by N-H···π, C-I···π and S2—O21··· π interactions instead of the classic O···H—N hydrogen bonds. The interactions were confirmed by HS analysis. Interaction energy calculations showed that the π interactions-based motifs play an important role in the supramolecular arrangement, contributing about 60% to the total energy of the lattice. DFT calculations showed that the energy of the C-I···π dimer is complemented with contributions of π···π stacking and N-H···π interaction between the primary amine and the thiazole aromatic ring.

Introduction

Compounds containing the 1,3-benzothiazolyl framework, see Figure 1, have found wide uses, particularly in such biological areas as antitumor, antiviral, and antimicrobial agents, in treatment of autoimmune and inflammatory diseases, among others [1,2]. They are also important precursors of optical materials, e.g., as dyes, fluorescence probes, and for the detection of photo-physical properties [1,3]. These compounds are also of interest for the study of liquid crystal properties [4]. They are also important precursors of optical materials, e.g., as dyes, fluorescence probes, and for the detection of photo-physical properties [1,3]. Study of liquid crystal properties [4] are also of interest. Moreover, these scaffolds have been utilized in industry as antioxidants, vulcanization accelerators, chemo-sensors for a range of analyses, as dopants in light-emitting organic electroluminescent devices, fungicides in leather and paper production, corrosion inhibitors in antifreeze formulations, and ultraviolet (UV) light stabilizers in textiles and plastics [5]. Consequences of the different environmental impacts of these high-production volume chemicals have been thoroughly assessed [5]. A particular well-studied 1,3-benzothiazolyl derivative, used mainly as a precursor is 2-hydrazinyl-1,3-benzothiazole, Bt-NH-NH$_2$, **1** (Scheme 1): a recent search, on 24/01/2020, of the REAXYS database [6] for this compound revealed more than 570 references to its use as a product in its own right and as a precursor of other 1,3-benzothiazolyl derivatives. Examples of the uses mentioned above for general 1,3-benzothiazolyl compounds are also found in the specific search of 2-hydrazinyl-1,3-benzothiazole, **1**. Compounds formed from **1** include the general formula derivatives Bt-NH-N=CHR$_1$ (R$_1$ = alkyl, aryl and heteroaryl) and its imino tautomer Bt-NH-NHCOR$_1$ and Bt-NH-NHSO$_2$R **2** (Scheme 1). The **2** derivatives (Scheme 1) have been less frequently studied, with the only reports dealing with syntheses and structures, including Hirshfeld surface and PIXEL calculations, of two derivatives of **2**, with (R = Ph and R = 3-O$_2$NC$_6$H$_4$) [7]. Further studies of the reactions of Bt-NH-NH$_2$, **1** with benzenesulfonyl chlorides, XC$_6$H$_4$SO$_2$Cl (X=2-O$_2$N-, 4-O$_2$N, 4-F, 4-Br), at 1:1 mol ratios have confirmed the general findings, with products, **2**, always obtained [8]. In contrast, the product isolated from the reaction using XC$_6$H$_4$SO$_2$Cl (X=4-I) was Bt-N(SO$_2$C$_6$H$_4$-4I)-NH$_2$, **3**, N'-(1,3-benzothiazol-2-yl)-4-iododbenzenesulfonohydrazide i.e., from reaction with the non-terminal nitrogen of the arenehydrazine unit, see Scheme 1. This reaction was indeed the only exception.

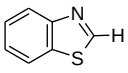

Figure 1. 1,3-benzothiazole, Bt-H.

[a] Herbert Fruchtl, Tanja van Mourik
University of St Andrews, School of Chemistry,
St Andrews KY16 9ST, Fife, Scotland, UK.
E-mail: herbert.fruchtl@st-andrews.ac.uk, tanja.vanmourik@st-andrew.ac.uk

[b] Lígia Rebelo Gomes
FP-I3ID, CEBIMED, Universidade Fernando Pessoa,
Praça 9 de Abril, 349, 4249-004 Porto, Portugal.
E-mail: lrgomes@ufp.edu.pt

[c] Lígia Rebelo Gomes
Departamento de Química e Bioquímica, REQUIMTE, Faculdade de Ciências da Universidade do Porto
Rua do Campo Alegre, 687, P-4169-007 Porto, Portugal.
E-mail: lrgomes@ufp.edu.pt

[d] John N. Low, James L. Wardell
University of Aberdeen, Department of Chemistry,
Old Aberdeen AB24 3UE, Scotland, UK.
E-mail: jnlow111@gmail.com, jms_wardell@yahoo.co.uk

[e] Alessandra C. Pinheiro, Marcus V. N. de Souza, James L. Wardell
Fiocruz–Fundacao Oswaldo Cruz, Instituto de Tecnologia em Farmacos – Farmanguinhos.
Sizenando Nabuco 100, Manguinhos, 21041-250, Rio de Janeiro, Brazil.
E-mail: ales.campbell@gmail.com, mvndesouza@gmail.com

Supporting information for this article is given via a link at the end of the document

The formation of the derivatives **2** from $ArSO_2Cl$ with Bt-NH-NH_2 follows the general findings for the frequently used direct-reactions of arylhydrazines with arenesulfonyl chlorides in the presence or absence of bases such as Et_3N or pyridine [9], i.e., that isolated products arise from reactions at the terminal nitrogen of the hydrazine unit. Very few exceptions have been reported in the literature; one example being the formation of $MeN(SO_2Ar)NH_2$ compounds from 1:2 mol reactions of $ArSO_2Cl$ and $MeNHNH_2$ in THF [10]. While there are a number of known R-$N(SO_2R)$-NH_2 compounds in the literature, these are formed by methods other than reactions of $RNHNH_2$ and RSO_2Cl, e.g., reactions of $ArSO_2NH$-NH_2 with activated sp^2 and sp^3 carbon-halogen compounds [11]. In a recent report [12], reactions of arenediazonium salts, ArN_2+X, with the reagent rongalite [$Na^+HOCH_2SO^{2-}\bullet 2H_2O$] produced well-characterized $ArNHNHSO_2Ar$ compounds, including where Ar=4-IC_6H_4. As such the question regarding the role of theI atom in the synthetic pathway and stabilization of the structure was raised. In order to determine the factors behind the unexpected formation of **3**, a structural and theoretical study has been carried out.

Results and Discussion

Molecular structure

The reaction between 2-hydrazinyl-1,3-benzothiazole and 4-$IC_6H_4SO_2Cl$ results in compound **3** (Scheme 1) rather than the expected Bt-NH-NH-$SO_2C_6H_4I$, **2**, with R= 4-IC_6H_4 as confirmed by Rx analysis. The molecular structure is depicted in Figure 2, together with the adopted numbering scheme, and 50% thermal ellipsoids. There are no unusual bonds or angles in the molecule [13]. The benzothiazole ring is planar and has a dihedral angle of 78.56(6)˚ with the C21 phenyl ring. The angle sum around N21 and around N22 is 352.99˚ and 321.14˚, respectively. The N21—N22 bond distance of 1.4192(17) Å is consistent with this type of bond involving planar and pyramidal N atoms [13]. The compound displays an intramolecular H -bond, involving the primary amine and the nitrogen atom of the thiazole ring, e.g. N22—H22A···N3 with H···N of 2.417(19) Å, N···A of 2.7098(19) Å and N—H···N angle of 100.9(15)º.

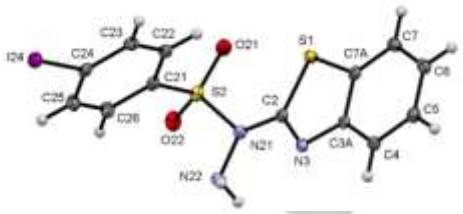

Figure 2. N-(1,3-benzothiazol-2-yl)-4-iodobenzene-1-sulfonohydrazide

Supramolecular structure

The presence of the primary amine and the sulfonyl group suggests that there should be strong N—H···N and N—H···O hydrogen bonds playing an important role in the supramolecular structure of the compound. Instead it is found that the supramolecular arrangement was driven by N–H···π, C–I···π, S=O···π, π··· π interactions and C—H···O/N hydrogen bonds.

In the following discussion, Cg_1 is the centroid of the thiazole ring, Cg_2 is the centroid of the benzothiazole phenyl ring, Cg_3 is the centroid of the phenyl group attached to the sulfone and Cg_4 is the centroid of the benzothiazole moiety (see scheme inserted in Tables 1 and 2 for Cg_1 to Cg_3). The N22—H22B···Cg_2 (-*x*,1-*y*,1-*z*), interaction forms a motif (**motif I**) that consists of a centrosymmetric dimer between two π-stacked benzothiazole rings, Figure 3a, Table 1. The molecules are also linked by the C24—I24···Cg_4 (1-*x*, 2-*y*,1-*z*), interaction to form another centrosymmetric dimer, **motif II** (Table 1, Figure 3b). These two dimers are linked alternately to form a chain which runs parallel to [110], Figure 3c. The S2—O21···Cg_3 (*x*, –1+*y*, *z*), interaction links the molecules into a chain, **motif III**, which runs parallel to the *y-axis* (Figure 3e and Table 1). There are weak C—H···N/O intermolecular hydrogen bonds in the structure (Table 1); the C5—H5···N3 (–*x*, –*y*+2, –*z*+1) hydrogen bond links the molecules into centrosymmetric dimers, making R_2^8 rings, **motif V** as shown in Figure 3f, and a chain is produced by the action of a glide plane at *y*=1/4 which runs parallel to the *c-axis,* (Figure 3g), due to the C6—H6···O22 (*x*, 0.5–*y*, 0.5+*z*) hydrogen bond, **motif VI**.

As mentioned above, in spite of having a primary amine and sulfonyl oxygen atoms as well as a nitrogen atom of the thiazole that could act as donors and acceptors for classic N–H···O/N hydrogen bonds, the supramolecular arrangement of **3** is driven by C–H···N and C–H···O hydrogen bonds and by dominant N–H···π and C–I···π interactions.

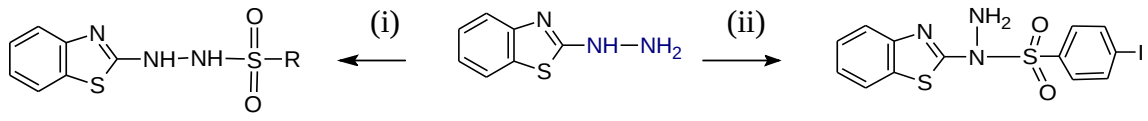

2 **1** **3**

Scheme 1. Reagents. (i) $XC_6H_4SO_2Cl$ (X = H, 2-F, 4-Br, 2-, 3- and 4-O2N; (ii) 4-IC_6H_4 SO_2Cl.

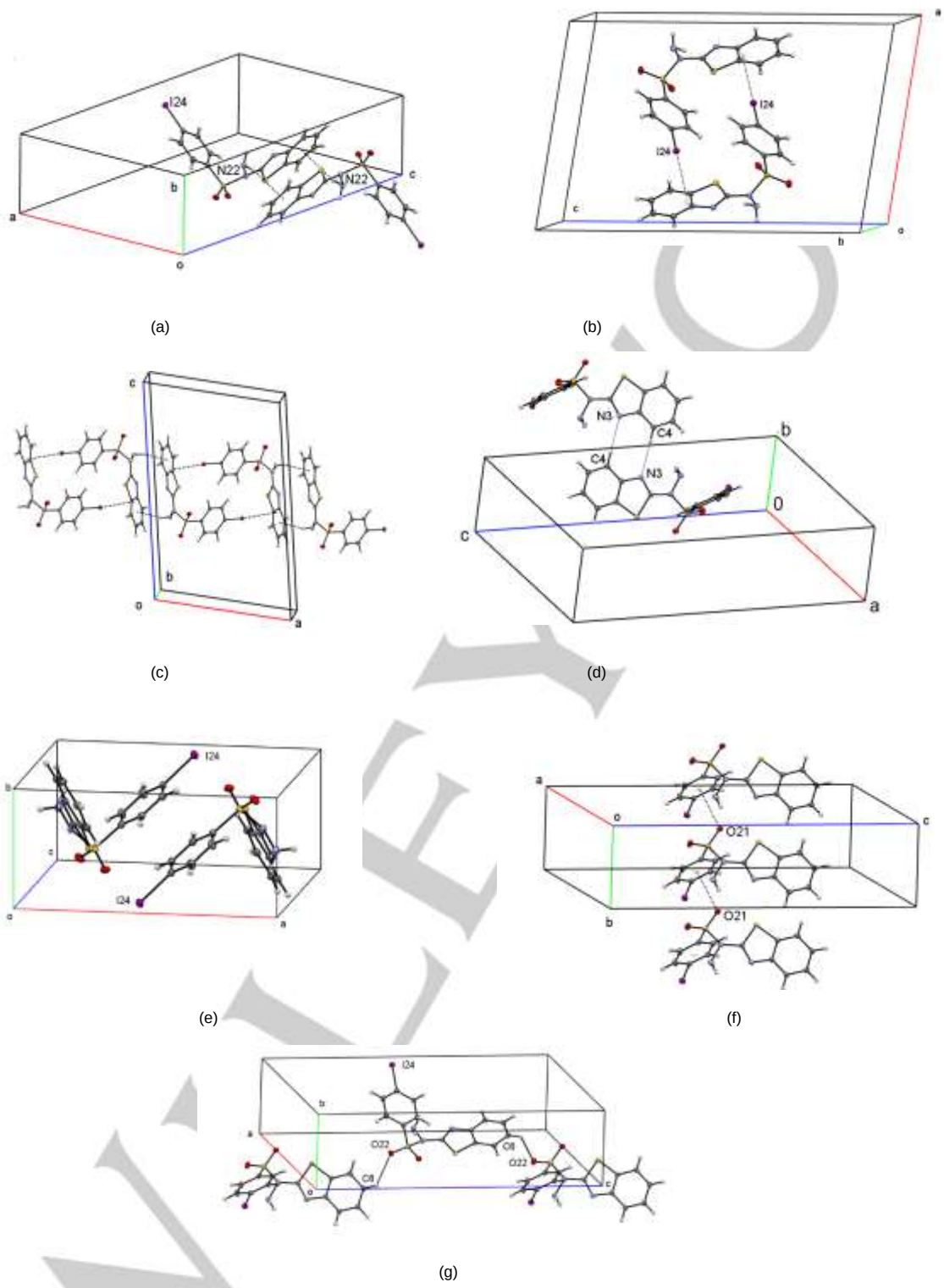

Figure 3. The supramolecular motifs for **3** and their energies. (a) **Motif I** relating molecule at x, y, z with that at *–x*, 1*–y*, 1*–z* having an E_{tot}=-53.4 kJmol^{-1}. Molecules are connected by N22–H22B ⋯ π intramolecular interactions. (b) **Motif II**, E_{tot}=-41.4 kJmol^{-1}, showing the dimer made by C24–I24⋯π interactions relating the *x, y, z* molecule with that placed at at 1*–x*, 2*–y*, 1*–z*. (c) The chain made by combination of **motif I** and **II**. (d) **Motifs III$_a$/III$_b$** , a chain made by S2—O21⋯ π interactions contributing with -40.6 kJmol^{-1} to the total energy, symmetry: x, 1+*y*, *z and x*, *–*1+ *y*, *z*. (e) Representation of **motif IV** (E_{tot}= -34.4 kJmol^{-1}), a dimer relating the molecule at *x, y, z* with the centrosymmetric partner located across the centre-of-symmetry at (0.5, 0.5, 0.5). (f) The N3⋯H4 – C4 H bond in **motif V**, contributing with -34.6 kJmol^{-1} for the lattice stabilization and (g) the chain made by **motifs VI$_a$/VI$_b$** (*x*, 0.5*–y*, *–*0.5+*z* and *x*, 0.5*–y*, 0.5+*z)* showing the O22⋯ H6 – C6 H bonds. Each of those motifs present an energy of -16.0 kJmol^{-1}.

Table 1. Intramolecular Intercations

Hydrogen bonds in (Å/º)				
D—H···A	D—H	H···A	D···A	D—H···A (º)
C4—H4···N3^{i}	0.95	2.60	3.5337 (19)	167
C6—H6...O2^{ii}	0.95	2.53	3.1817 (15)	126

Y—X/H …Ring interactions in (Å/º)					
Y—X/H	Cg	X···Cg	X···Perp	Y-H···Cg (º)	Y···Cg
C24—I24	Cg_1 (1-x,2-y,1-z)	3.6231(6)	3.367	147.78(4)	5.5091(16)
C24—I24	Cg_2 (1-x,2-y,1-z)	3.4941(6)	3.354	153.20(4)	5.4458(16)
C24—I24	Cg_4 (1-x,2-y,1-z)	3.3750(5)	3.342	156.29(4)	5.3590(16)
S2—O21	Cg_3 (x,-1+y,z)	3.2715(13)	3.256	119.88(6)	4.1759(8)
N22—H22B	Cg_2 (-x,1-y,1-z)	2.90(2)	-2.68	140.8(18)	3.6066(15)

Ring…Ring interactions in (Å/º)						
CgI	Cg	Cg···Cg	α (º)	CgI perp	CgJ perp	Slippage
Cg_1	Cg_1 (-*x*,1-*y*,1-*z*)	3.6642	0.00(6)	-3.3790(5)	-3.3789(5)	1.417
Cg_1	Cg_4 (-*x*,1-*y*,1-*z*)	3.8078	0.95(5)	-3.3776(5)	-3.4014(4)	1.712
Cg_4	Cg_1 (-*x*,1-*y*,1-*z*)	3.8078	0.95(5)	-3.4014(4)	-3.3776(5)	1.758

Cg_1 is the centroid of the 5-membered ring and Cg_2 is the centroid of the six membered ring of the benzothiazole moiety; Cg_3 is the centroid of the phenyl ring attached to S2 and Cg_4 is the centroid of the benzothiazole moiety, α is the angle between the mean planes of the rings defined by CgI and CgJ.

Symmetry codes: (i), *-x*,*-y*+2, *-z*+1; (ii) *x*, *-y*+1/2, *z*+1/2

There are two structures in the Cambridge Structural Database [14] that contain a sulfonylhydrazino moiety similar to that of the title compound: N-((4-methylphenyl)sulfonyl)hexanehydrazide, HUNLOS, [15] which contains 2 molecules in the asymmetric unit and methyl 4-((1-((4-methylphenyl)sulfonyl)hydrazino) carbonyl)benzoate WELNAE, [16] (Figure 4). In HUNLOS there are classical intermolecular hydrogen bonds involving the amino hydrogen atoms and the sulfonyl oxygen atoms, which link the molecules into chains. In addition, there are two intermolecular C—H···π interactions. In WELNAE there is one classical N—H···O hydrogen bond of the amino group to one of the sulfonyl O atoms and a short intramolecular contact via the second amino hydrogen to an oxygen of the sulfonyl group. These interactions are different from those observed in the title compound, where a short intramolecular contact to the N atom of the benzothiazole ring exists.

The C—X···π interactions (X = F, Cl, Br and I), in general, have been well studied experimental and theoretically, with extensive surveys of crystallographic databases also employed [17-20]. Of interest, evidence has been found for such interactions occurring in solution [17, 20], which suggests a possible pre-assembly of C—I···π linked dimers in solution in our reactions prior to crystallization of compound **3**.

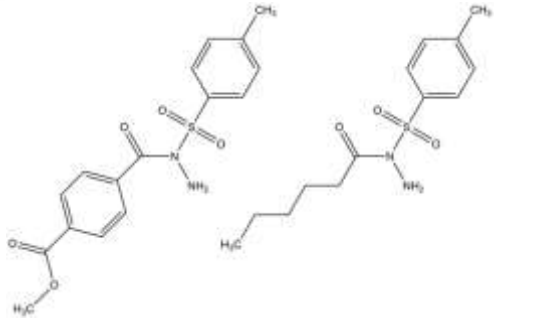

Figure 4. Methyl 4-((1-((4-methylphenyl)sulfonyl)hydrazino)carbonyl)benzoate [16] and N-((4-Methylphenyl)sulfonyl)hexanehydrazide [15].

With respect to the C—I···π interaction, a search of the CSD showed that there were 584 structures displaying short C—I···π contacts, both organic (524) and organometallic (60), with distances ranging from 3.00Å to 3.85Å and an angular range of 130° to 180°. Of these only OCENET, 6,6-difluoro-3-iodo-5-methyl-5,6-dihydro-7,6-[1,3]benzothiazolo[3,2-*c*][1,3,2]benzodiazaborinine [21], involves a C—I···π interaction with a benzothiazole moiety. In this case the shortest contact is between the I atom and the centroid of the benzothiazole phenyl ring with an I···centroid distance of 3.6436(8) Å, an angle at I of

154.47(6)˚ and a C···centroid distance of 5.616(2) Å. These values are slightly longer than those presented for the C—I···π interaction in **3**.

There are 76 structures with distances ranging from 2.5Å to 3.5Å and an angular range of 130˚ to 180˚ in the CSD that contain N—H···π interactions, three of which are simple (benzothiazol-2-yl)hydrazine compounds**.** There are 567 structures with S=O···π interactions, with distances ranging from 2.5Å to 3.5Å and an angular range of 110˚ to 180˚, none of which involve benzothiazole moieties.

Interaction Energies and Hirshfeld surfaces analysis

In order to gain a better insight into the energy levels and main motifs contributing to stabilization of the supramolecular structure, the energies for intermolecular interactions in the crystal were calculated using Crystal Explorer [22] with a CE-B3LYP model. According to Mackenzie et al. [23], the mean absolute deviation of CE-B3LYP model energies from DFT values is about 2.4 kJ mol^{-1} for pairwise energies that span a range of 3.75 MJ mol^{-1}. This is due to the application of scaling factor corrections to the calculated energies, which were determined by fitting to counterpoise-corrected DFT calculations. This is a model energy formalism similar to Gavezzotti's PIXEL approach [24] and allows calculations to be made on coordination compounds and organic structures incorporating iodine atoms.

In table 2 the main sub-structural molecular motifs are given with a cut-off value of -10.0 $kJmol^{-1}$. The calculated total energy of interaction by the CE-B3LYP model applied according to Mackenzie et al. [23] was 316.9 $kJmol^{-1}$ and the identified motifs contribute an energy of -309.4 $kJmol^{-1}$ towards the stabilization of the supramolecular arrangement, which is about 97% of the total energy.

The most stable motif is **motif I** relating a molecule at *x, y, z* with that positioned at *–x*, 1*–y*, 1*–z,* see Figure 3(a), with E_{tot}=-53.4 $kJmol^{-1}$, which makes a significant contribution to the overall energy of the pair, from both Coulombic and dispersion terms, with the dispersion about 16 $kJ.mol^{-1}$ higher (Table 2). The same reasoning applies to **motif II** (Figure 3(b)), relating the molecule at *x, y, z* with that placed at 1*–x*, 2*–y*, 1*–z* and for which E_{tot} is -41.4 $kJmol^{-1}$, but here, the Coulombic term is smaller (about 8 $kJmol^{-1}$). In **motif II**, as identified before, a short contact between the iodine atom and the thiazole ring of the benzothiazole is observed, suggesting the existence of the already identified I···π interaction, see geometrical parameters in Table 1 and energies in Table 2. This means that along the [110] direction, (Figure 3c), the N22–H22B···π and the C24–I24···π interactions are the real contributors to the molecular chain. With a total energy of -40.6 $kJmol^{-1}$, **motifs IIIa/IIIb** (Figure 3d) relate molecules via a S2—O21···π interaction. In **motifs III** the dispersion energy is double the Coulombic energy, pointing again to the importance of electronic delocalisation within the crystalline net for its stabilization. The chains made by the combination of **motifs I** and **II** are connected by N3···H4–C4 /C4–H4···N3 interactions identified as **motif V** as depicted in Figure 3(e) with the corresponding energy, see table 2. The computed energies of molecular pairs also indicate another substructural motif, which is energetically more relevant than **motif V**, although it does not show atom···atom close contacts smaller than the sum of the covalent radii. This motif is identified as **motif IV** (figure 3d and relates the molecule at *x, y, z* with the centrosymmetric partner located in the neighbouring unit cell. The existence of **motif IV** of **3** cannot be explained in terms of hydrogen bonds or other contacts, considering that any measurable interaction is extremely long (> 2.8 Å). To understand the factors contributing to the stabilization of the pairs, the analysis of the terms contributing to the total CE-B3LYP interaction energy is of great help. In **motif IV** the dispersive contribution is significantly higher than the electrostatic contribution, showing that the disposition of the molecule at 1*–x*, 1*–y*, 1*–z* in relation to the molecule at *x, y, z* favours the electronic dispersion. Finally, the C-H···O hydrogen bond (**motif** pair **VIa/VIb**), represented in Figure 3f, contributes 16.0 $kJmol^{-1}$ to the total energy of the lattice, suggesting that H-bonding is not a dominant energetic contribution to the stabilization of the supramolecular structure of **3**.

Hydrogen bonds and other interactions can be observed through Hirshfeld surface (HS) analysis using the *CrystalExplorer* program [22], which allows the visualization of interactions within the crystalline structure. Assigning d_e and d_i as the external and internal distances of an atom to the Hirshfeld surface and normalizing these pairs of values to the van der Waals (VdW) radii of the corresponding atoms results in the so called d_{norm} surface. Interactions smaller than the sum of the VdW radii of the two atoms result in a negative value, highlighted on the surface as red spots.

Figure 5 shows the red areas for the N22–H22B···π, C24–I24···π, N3···H4–C4 and the O22···H6–C6 contacts, see table 1 for geometric parameters, indicating that the atom···atom distances involved are shorter than the sum of the VdW radii. Figure 6 shows the total 2D (2-dimensional) fingerprint plot of **3**, where it can be notice the lack of typical spikes pointing southwest due to the absence of short N/O···H contacts typical of strong classic hydrogen bonds. The only sharp section in the plot corresponds to pairs of spikes ending at coordinates (d_e, d_i) ≅ (2.1, 1.2) Å/ (d_e,d_i) ≅ (1.2, 2.1) Å. These appear for the I···H close contacts, but they are larger than the sum of van der Waals radii, showing that there are no I···H interactions. Another pair of spikes appear at the coordinates set (d_e,d_i) ≅ (1.0, 1.4) /(d_i,d_e) ≅ (1.4, 1.0) relating N to H contacts. The spiky ends of the I···C close contacts are covered by total 2D print surface, but they appear when the I···C/C···I close contacts are discriminated at (d_e,d_i) ≅ (1.8, 1.5) Å and (d_e,d_i) ≅ (1.5, 1.8) Å. The results suggest that the crystal structure of **3** is driven mainly by unusual N–H···π and C–I···π interactions.

The percentages of relevant contacts are: H···H (30.1%); O···H/ H···O (16.1%); C···H/ H···C (12.8%); I···H/ H···I (9.7%); C···I/ ···C (8.5%); N···H/ H···N (4.3%); S···H/ H···S (3.8%) and N···C/ C···N (2.6%).

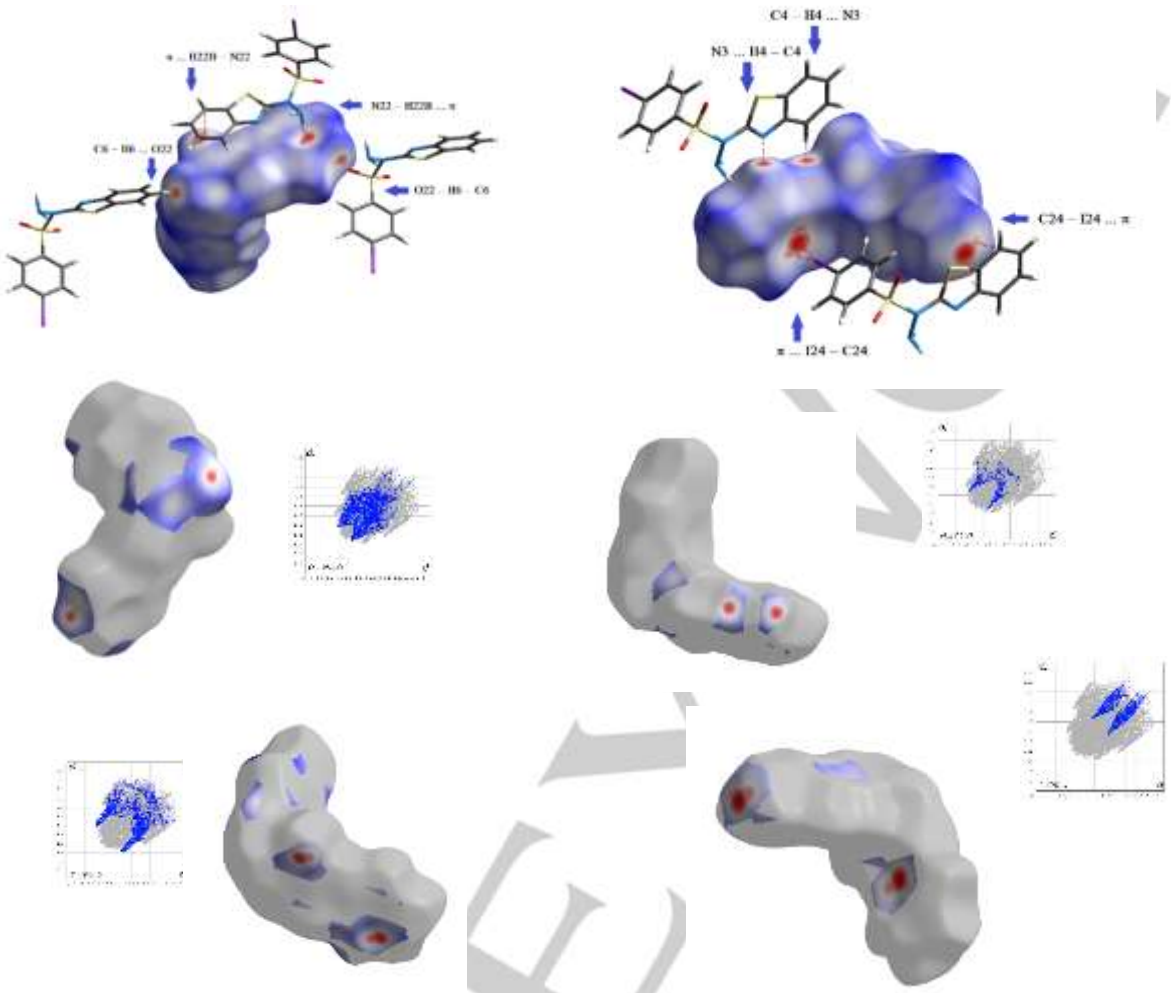

Figure 5. Views of the Hirshfeld surface mapped over d_{norm} 1, showing red areas pointing for atom···atom close contacts. The contacts are identified in the figure.

Table 2 - List of the intermolecular interaction energies for molecular pairs in **3**

Sub Structural Motifs	Symmetry code	Contacts	E_{tot} (kJ.mol^{-1})	E_{coul} (kJ.mol^{-1})	E_{pol} (kJ.mol^{-1})	E_{disp} (kJ.mol^{-1})	E_{rep} (kJ.mol^{-1})
I	–*x*, 1–*y*, 1–*z*	N22 – H22B ··· π π ··· H22B – N22	-53.4	-37.8	-3.5	-54.3	42.2
II	*1* -*x*, 2–*y*, 1–*z*	π ··· I24 –C24 C24 – I24 ··· π	-41.4	-49.4	-2.7	-57.5	68.1
IIIa **IIIb**	*x*, 1+ *y*, *z* *x*, –1+*y*, *z*	S2—O21··· π	-40.6	-21.4	-3.0	-42.6	26.4
IV	1– *x*, 1–*y*, 1–*z*	- - - -	-34.4	-26.6	-2.9	-39.3	34.4
V	– *x*, 2–*y*, 1–*z*	N3···H4 – C4 C4 – H4 ··· N3	-22.6	-16.3	-2.9	-25.3	21.8
VIa **VIb**	*x*, 0.5–*y*, –0.5+*z* *x*, 0.5 –*y*, 0.5+*z*	O22··· H6 – C6	-16.0	-9.3	-1.3	-13.9	8.5

B3LYP/ DGDZVP electron densities were used. Scale factors, *k*, for energy values were applied to the table values (1.057, 0.740, 0.871 and 0.618 for k_{ele}, k_{pol}, k_{disp} *and* k_{rep}, respectively) [22].

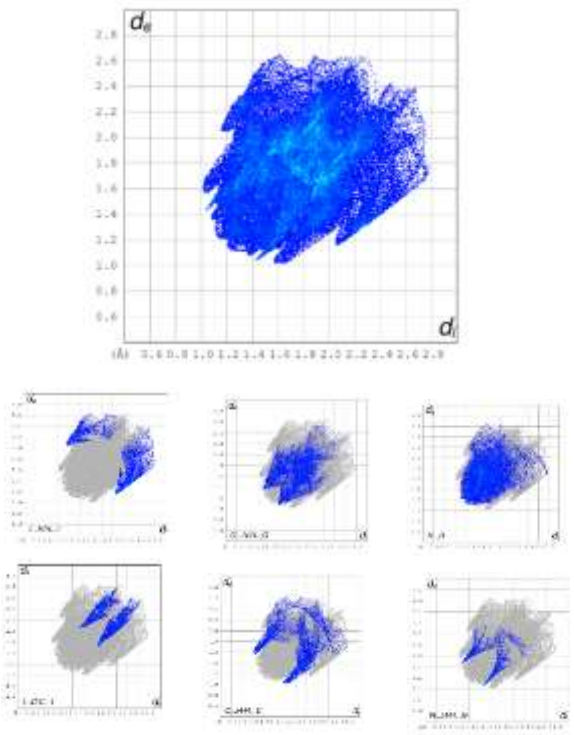

Figure 6. FP plots for **3**. The absence of spikes is indicative of the lack of short N/O···H contacts typical of the strong classic hydrogen bonds. Only a pairs of spikes pointing to south-west ending at coordinates (d_e, d_i) ≅ (2.1, 1.2) Å and (d_e, d_i) ≅ (1.2, 2.1) Å appear for the I···H close contacts; these are larger than the sum of the Van der Waals radii, showing there are no I···H interactions. In contrast, the smaller I···C close contacts are covered by the main surface but appear when the I···C /C…I close contacts are discriminated as spikes ending at (d_e, d_i) ≅ (1.8, 1.5) Å and (d_e, d_i) ≅ (1.5, 1.8) Å.

Theoretical calculations

To attempt to explain the preference for reaction route ii) instead of the normally observed route i) observed for **3**, geometry optimizations were performed on monomers, both for compound **3** (the product with the benzothiazole on the non-terminal N of the hydrazide), see Scheme 1, and for the expected product **2** (with the benzothiazole on the terminal hydrazide nitrogen). The geometries were extracted from the .cif files of **3** and from the .cif files of a related compound of **2** (with the benzothiazole attached to the terminal hydrazide nitrogen with R=PhF). In the latter case, the F atom was replaced by an I atom. The optimised structures were confirmed as minima by frequency calculations. It was found that monomer **2** is more stable by 9.1 kJmol^{-1} compared to **3**. Vibrational and thermal corrections have very little effect (enthalpy change: 8.9 kJmol^{-1}; free energy change: 10.5 kJmol^{-1}). Thus, a difference in the monomer energy cannot explain why this molecule crystallises with the benzothiazole on the first hydrazine nitrogen, suggesting that the experimental preference for product **3** is probably related to the reaction mechanism.

To further study the main interactions present in the structure of **3,** a dimer with C—I···π interactions was extracted from the .cif file of 3 and energy calculations were performed without geometry optimization. Figure 7 shows the structure of the C—I···π-bonded dimer extracted from the crystal structure as described before. The CP-corrected interaction energy of the C-I··· π -bonded dimer was found to be -47 kJmol^{-1}. In this dimer, the halogen points to the middle of the C=C bond separating the 5- and 6-ring. NBO analysis reveals that the halogen is positively charged (+0.160). A molecular electrostatic potential (MEP) map of the monomer (figure 8) shows that the charge distribution around the iodine is anisotropic and shows a clear σ-hole at the extension of the C-I bond, indicating the molecule's ability to form halogen bonds. When a model system consisting of an iodomethyl molecule located above a benzothiazole molecule is optimised, the iodine points to the middle of the 6-membered ring. This suggests that an additional attraction is moving the two iodobenzene fragments closer together in the dimer formed in **3**. This attraction is presumably π-π stacking between the two iodobenzene fragments. To investigate this further, the interaction energy of two iodobenzene molecules at the same position as in the C—I··· π-bonded dimers was calculated. This provided a value of -15 kJmol^{-1}.

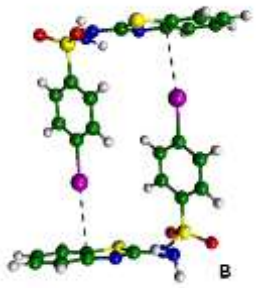

Figure 7. The C-I···π dimer extracted from the crystal structure

In addition, the dimer might have an additional stabilisation from the NH_2 group interacting with the six-ring of the benzothiazole unit. The CP-corrected interaction energy of a model structure, consisting of an NH_3 molecule located above a benzothiazole molecule (with the atoms at the positions of the crystal structure), was calculated to be 10 kJmol^{-1}, providing an estimate of this interaction to the stability of the crystal structure based on the C-I···π bonded dimer. Thus, the combination of the N—H ···π and C-I ···π interactions, with some π···π stacking, contributes to the stabilization of this dimer, though the sum of these interactions is not sufficient to compensate for the loss of the O···H—N hydrogen bonds present in compound **2.**

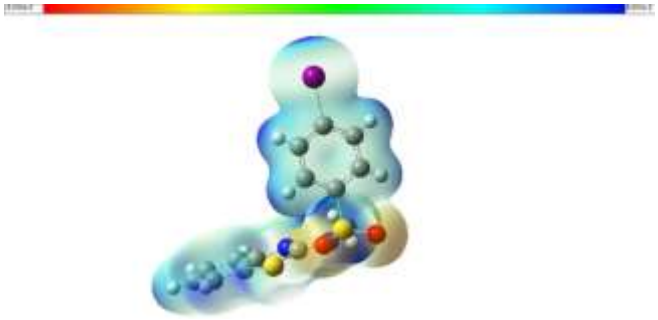

Figure 8. Molecular electrostatic potential (mapped on the 0.006 e^-/au^3 electron density surface) of compound 3. Blue and red represent positive and negative regions of electrostatic potential, respectively (from 0.08 to -0.0.8 E_h/e^-).

Conclusions

The product **3** of the reaction of Bt-NH-NH_2 with Iodobenzenesulfonyl chloride is very unusual, in the sense that the benzothiazole moiety is not attached to the terminal hydrazide nitrogen, as is commonly observed for similar compounds synthesized under the same conditions. The crystal structure of **3** is stabilised by that the dominant C—I···π, N—H···π and S=O···π interactions instead of the expectable N—H···O H bonds. These highlight the importance of the X···π ccontacts in aromatic systems.

Experimental Section

Synthesis

A solution of 2-hydrazinyl-1,3-benzothiazole (1.66 g, 1 mmol) and 4-iodobenzenesulfonyl chloride (3.00 g, 1mmol) in EtOAc (20mL) was refluxed for 1 h. The reaction mixture was washed with water, the organic layer collected, dried over magnesium sulphate and rotary evaporated. The residue was recrystallized from an ethanol solution. Yield 76%, m.p. 190-192 °C. The reaction was repeated in MeOH, both under reflux and at room temperature, and also in EtOAc in the presence of Et_3N, and the identical product was isolated in all cases. The recrystallized yield in each case was greater than 70 %. Another experiment was carried out on an NMR scale, using 2-hydrazinyl-1,3-benzothiazole (8.5 mg) and 4-iodobenzenesulfonyl chloride (3 mg) in MeOH-d_4 (1.5 ml). After leaving sealed for two days, the ^{1}H NMR spectrum indicated that the sole detectable product was the title compound; as is known, the limits of detection by NMR is in the region of 5%.The sample used in the structure determination was obtained by slow evaporation of an ethanol solution at room temperature after one day.

IR (cm^{-1}): 3338 (small and sharp), 1611, 1567, 1487, 1441, 1364, 1260, 1168, 1086, 1008, 956, 878, 811, 768, 732, 678.

^{1}H NMR (400 MHz, DMSO-d6): 8.03 (2H, *d*, J = 8.8Hz), 7.79 (1H, *m*), 7.87 (2H, *d*, J = 8.8Hz), 7.65 (1H, *br. d*, J = ca. 8Hz), 7.37 (1H, *br.d.t*, J = ca 8 & 1Hz), 7.25 (1H, *br.d.t*, J = ca 8 & 1Hz).

^{13}C NMR (100 MHz, DMSO-d6): 165.24, 151.00, 138.09, 136.45, 132.17, 130.29, 129.46, 127.76, 126.12, 123.53, 121.56, 120.80, 103.27. Accurate mass: found [M + H] = 431.9335: calculated 431.9337

.

Crystal structures

The title compound crystallised in the monoclinic spacegroup, $P2_1/c$, with Z = 4. Data were collected on a Rigaku diffractometer using Mo radiation, λ = 0.71075, at 100K. Cell dimensions were determined from 10766 reflections. Cell dimensions: *a*=12.8234 (2) Å, *b*=5.5996(1) Å, *c* = 20.4759(3) Å, β = 100.878(1)°, see Table 1 in supplementary information. Refinement was carried out using full matrix least squares, the final R-factor being 0.0143 for 3311 reflections. H atoms attached to C were treated as riding atoms. Amino hydrogen atoms were refined based on their positions in a difference map. These hydrogen atoms show up very clearly and exactly at their refined positions on a final difference map.

Energy frameworks and Hirshfeld surfaces mapped over d_{norm} and two-dimensional fingerprint plots of the title compound were calculated using CrystalExplorer17.5 [22]

Theoretical calculations

Calculations were carried out on monomers and dimers extracted from the crystal structure of **3** and a related compound **2** (with the benzothiazole attached to the terminal hydrazide nitrogen with R=PhF), using the PBE0 hybrid functional [25], augmented with the D3BJ dispersion term [26], employing the def2-TZVP basis set [27]. Interaction energies were corrected for basis set superposition error (BSSE) by using the counterpoise (CP) procedure [28]. All calculations were carried out with Gaussian 16 [29].

Acknowledgements

The authors thank the staff at the National Crystallographic Service, University of Southampton for the data collection and advice [30]. TvM and HF thank EaStCHEM for access to the EaStCHEM Research Computing Facility.

Supporting information

CCDC 2123865 contains the supplementary crystallographic data for this paper. These data can be obtained free of charge from The Cambridge Crystallographic Data Centre via http://www.ccdc.cam.ac.uk/data_request/cif. The details of the crystal structure determination in cif format are also available in the online version (https://doi.org/10.1515/znb-2020-0126).

Author contributions

All the authors have accepted responsibility for the entire content of this submitted manuscript and approved submission.

Research funding: None declared.

Conflict of interest statement: The authors declare no conflicts of interest regarding this article.

Keywords: sulfonohydrazide• benzotiazole• iodobenzene • π-interactions• intermolecular forces

[1] Benzothiazole: Preparation, Structure and Uses, (ed.A. Heijstek), Nova Science Publishers Inc, NY, USA, 2020. ISBN: 9781536175486.

[2] a) M. B. Elamin, A. A. E. S. A. Elaziz, E. M. Abdallah, *Int. J. Res. Pharm. Sci*. **2020**, *3*, 3309-3315; b) N. Pathak, E. Rathi, N. Kumar, S. G Kini, C. M. Rao, *Mini Rev Med Chem*. **2020**, *20*, 12-23; c) M. Asif, M. Imran, *Mini. Rev.Org. Chem*. **2021**, *18*, 1086-1097.

[3] a) M. R. Maliyappa, J. Keshavayya, N. M. Mallikarjuna, I. Pushpavathi, *J. Mol. Struct*. **2020**, 1205, 127576; b) N. P. Thekkeppat, M. Lakshmipathi, A. S. Jalilov, P. Das, A. Malik, P. Peedikakkal, S. Ghosh, *Cryst. Growth Des*. **2020**, *20*, 3937–3943.

[4] K.-L. Foo, S.-T. Ha, G.-Y. Yeap, *Phase Trans.* **2022**: online. DOI: 10.1080/01411594.2021.2023745

[5] C. Lioa, U. J. Kim, K. Kannan, *Environ.Sci.Tchnol*, **2018**, *52*, 5007-5026.

[6] REAXYS, Elsevier, 2022.

[7] a) T. C. Baddeley, M. V. N. de Souza, J. L. Wardell, M. M. Jotani, E. R. T. Tiekink, *Acta Cryst.* **2019**, *E75*, 516–523; b) A. Morscher, M. V. N. de Souza, J. L. Wardell, W.T. A. Harrison, *Acta Cryst*. **2018**, *E74*, 673–677.

[8] L. R. Gomes, J. N Low, A. C. Pinheiro, M. V.N. de Souza, J. L. Wardell, unpublished, to be reported. (CCDC 2125105, 2124146, 2123875 and 2123876).

[9] Y. Zhang, C. Huang, X. Lin, Q. Hu, B. Hu, Y. Zho, G. Zhu, *Org. Lett*. **2019**, *21*, 2261 -2264.

[10] a) R. T. Hrubiec, K. Shyam, L. A. Cosby, A. C. Sartorelli, *J. Med. Chem*. **1986**, *29*, 1777-1779; b) H. G. Aslan, N. Karacan, *Med.Chem.Res*. **2013**, *22*, 1330–1338.

[11] a) K. Yang, J.-J. Gao, S-H. Luo, H.-Q. Wu, C.-M. Pang, B.-W. Wang, X.-Y. Chen, Z.-Y. Wang, *RSC Adv*, **2019**, *9*, 519917 and refs therein, b) T. J. Donohoe, J. F. Bower, J. A. Basutto, L. P. Fishlock, P. A. Procopiou and C. K. A. Callens, *Tetrahedron*, **2009**, *65*, 8969 – 8990.

[12] M. Wang, B.-C. Tang, J.-G. Wang, J.-C. Xiang, A.-Y. Guan, P.-P. Huang, W.-Y. Guo, Y.-D. Wua, A.-X. Wu, *Chem. Commun.* **2018**, *54*, 7641-7644.

[13] F.A. Allen, O. Kennard, D. G. Watson, L. Brammer, A. G. Orpen, R. Taylor, *J. Chem. Soc.Perkin Trans. II,* **1987,** S1-S19.

[14] C. R. Groom, I. J. Bruno, M. P. Lightfoot and S. C. Ward, *Acta Cryst*. **2016**. B72, 171-179

[15] K. Namba, I. Shoji, M. Nishizawa, K. Tanino, *Organic Letters* **2009,** *11*(21), 4970-4973.

[16] Y. Iwai, T. Ozaki, R. Takita, M. Uchiyama, J. Shimokawa, T. Fukuyama, *Chem. Sci.*, 2013, **4**, 1111-1119.

[17] H. Sun, A. Horatscheck, V. Martos, M. Bartetzko, U. Uhrig, D. Lentz, P. Schmieder, M. Nazaré, *Angew. Chem. Int. Ed*. **2017**, 56, 6454-6458, and references therein

[18] M. D. Prasanna, T.N. Guru Row, *Cryst. Eng*. **2000**, 3,135-154.

[19] D. Mitra, N. Bankoti, D. Michael, K. Sekar, T. N. Guru Row, *J. Chem. Sci*. **2020**, 132, 1-11.

[20] J. Jian, J. Poater, P. B. White, C. J. McKenzie, F. M. Bickelhaupt, J. Mecinović, *Org. Lett*. **2020**, 22, 7870–7873.

[21] Sheng-Ming Tseng, Chi-Min Chao, Kai-Hsin Chang, Chi-Sheng Wen, Tai-Che Chou, Tsung-Lun Tsai, Ting-Wen Wu, Xiao-Ci Haung, Jun-Qi Liu, Cheng-Hsien Hung, Kuan-Miao Liu, Pi-Tai Chou, *ChemPhotoChem*, **2021.**

[22] M. J. Turner, J. J. McKinnon, S. K. Wolff, D. J. Grimwood, P. R. Spackman, D. Jayatilaka, M. A. Spackman, *CrystalExplorer* Version 17, **2017,** University of Western Australia.

[23] C. F. Mackenzie, P. R. Spackman, D. Jayatilaka, M. A. Spackman. *IUCrJ*, **2014**, *4*, 575–587.

[24] A. Gavezzotti, *New J. Chem*. **2011**, *35*, 1360-1368; (b) A. Gavezzotti, *J. Phys.Chem,* **2003**, *B107*, 2344.

[25] C. Adamo, V. Barone, *J. Chem. Phys*. **1999**, *110*, 6158-6169

[26] S. Grimme, S. Ehrlich, L. Goerigk, *J. Comp. Chem.* **2011**, *32*, 1456-1465.

[27] A. Schaefer, C. Huber, R. Ahlrichs, *J. Chem. Phys*. **1994**, *100*, 5829-5835.

[28] S. F. Boys, F. Bernardi, *Mol. Phys*. **1970**, *19*, 553-566.

[29] Gaussian 16, Revision C.01, M. J. Frisch, G. W. Trucks, H. B. Schlegel, G. E. Scuseria, M. A. Robb, J. R. Cheeseman, G. Scalmani, V. Barone, G. A. Petersson, H. Nakatsuji, X. Li, M. Caricato, A. V. Marenich, J. Bloino, B. G. Janesko, R. Gomperts, B. Mennucci, H. P. Hratchian, J. V. Ortiz, A. F. Izmaylov, J. L. Sonnenberg, D. Williams-Young, F. Ding, F. Lipparini, F. Egidi, J. Goings, B. Peng, A. Petrone, T. Henderson, D. Ranasinghe, V. G. Zakrzewski, J. Gao, N. Rega, G. Zheng, W. Liang, M. Hada, M. Ehara, K. Toyota, R. Fukuda, J. Hasegawa, M. Ishida, T. Nakajima, Y. Honda, O. Kitao, H. Nakai, T. Vreven, K. Throssell, J. A. Montgomery, Jr., J. E. Peralta, F. Ogliaro, M. J. Bearpark, J. J. Heyd, E. N. Brothers, K. N. Kudin, V. N. Staroverov, T. A. Keith, R. Kobayashi, J. Normand, K. Raghavachari, A. P. Rendell, J. C. Burant, S. S. Iyengar, J. Tomasi, M. Cossi, J. M. Millam, M. Klene, C. Adamo, R. Cammi, J. W. Ochterski, R. L. Martin, K. Morokuma, O. Farkas, J. B. Foresman, and D. J. Fox, Gaussian, Inc., Wallingford CT, **2016.**

[30] S. J. Coles, P. A. Gale, *Chem. Sci* **2012**, *3*(3), 683-689.

10.1002/zaac.202200087

WILEY-VCH

FULL PAPER

When Bt-NH-NH_2 was allowed to react with 4-Iodophenyl sulfonyl chloride the unexpected product isolated was the titled compound as confirmed by Rx-analysis. The determination of the crystal structure revealed that the definition of the arrangement was driven by N—H···π, C-I···π and S2—O21··· π interactions instead of the classic O···H—N hydrogen bonds. Interaction energy calculations showed that the π interactions based motifs play an important role in the supramolecular arrangement contributing about 60% to the total energy of the lattice.

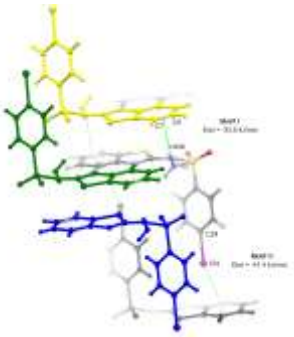

Lígia R. Gomes, Herbert. Früchtl, John N. Low,* , Tanja van Mourik, Alessandra C. Pinheiro, Marcus V. N. de Souza, James L. Wardell*

Page No. – Page No.

Crystal structure of N-(1,3-benzothiazol-2-yl)-4-iodobenzene-1-sulfonohydrazide: the importance of unusual N-H···π and I···π interactions on the supramolecular arrangement.

10.1002/zaac.202200087

WILEY-VCH